ChemComm

Accepted Manuscript

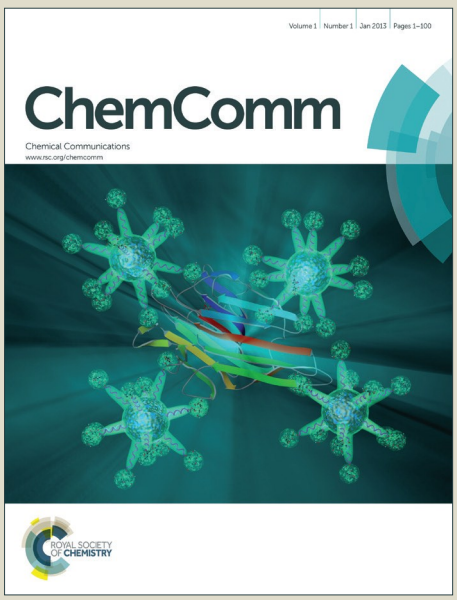

ROYAL SOCIETY OF CHEMISTRY

www.rsc.org/chemcomm

ChemComm

RSCPublishing

FEATURE ARTICLE

Mesoscale modelling of environmentally responsive hydrogels: Emerging applications

Cite this: DOI: 10.1039/x0xx00000x

Peter D. Yeh[a] and Alexander Alexeev[a]*

Received 00th January 2015,
Accepted 00th January 2015

DOI: 10.1039/x0xx00000x

www.rsc.org/chemcomm

Stimuli-sensitive hydrogels are an exciting class of materials with widespread potential for use in engineering and biomedical applications. The design of advanced functional devices using hydrogels requires an in-depth understanding of the physics and behaviour of such materials. While theoretical tools exist, they are often limited to simple cases. Thus, computational methods are necessary to model the complex unsteady physics of hydrogels with high fidelity. Mesoscale modelling is an emerging approach that enables simulations of polymeric structures at length and time scales in between those of molecular dynamics and continuum methods. In this feature article, we review various computational approaches to model responsive hydrogels and specifically focus on dissipative particle dynamics (DPD), a particle-based mesoscale method. We discuss several approaches for modelling cross-linked polymer networks in DPD, and we describe recent applications of DPD to modelling hydrogel systems.

1. Introduction

Stimuli-responsive polymers are smart materials that exhibit large-scale changes in their properties in response to specific environmental stimuli. Such external stimuli include changes in temperature,[1-9] pH,[10-14] humidity,[15-17] light intensity,[18-20] electric and magnetic fields,[21-26] and others.[22, 26-29] Some smart polymers have been developed to respond to multiple stimuli.[30-32] Responsive behaviour has been demonstrated for a wide variety of structures and molecular architectures, including polymer brushes, colloids, thin films, synthetic membranes, hydrogels, and micelles.[33]

Out of these different types of smart materials, responsive hydrogels have attracted significant attention due to their ability to undergo volume phase transitions depending on the environment, directly converting chemical energy into mechanical work. Thus, hydrogels, which are chemically or physically cross-linked polymer networks immersed in a solvent, are naturally suited for engineering applications that require mechanical signalling and actuation. Indeed in recent years, responsive hydrogels have been synthesized and demonstrated for the use in applications such as bio-sensors,[34-36] tissue engineering,[37] soft robotics,[23, 38, 39] and drug delivery.[40-43]

Fig. 1 demonstrates the utility of a responsive hydrogel as a self-propelled walker.[23] The walker has dual responsive appendages composed of cationic and anionic polyelectrolyte gels immersed in NaCl solution. When an external electric field is applied, the gel legs bend (Fig. 1a) and cause the walker to propel forward. Furthermore, applying a periodically changing electric field leads to a periodic "pulling" and "pushing" motion against the substrate, ultimately resulting in a unidirectional walking motion. Fig. 1b shows the sequence of steps that are performed after each switch in electric field direction. This exciting example illustrates how a responsive hydrogel with a relatively simple design and control can be effectively employed as a biomimetic actuator in soft robotics.

Microscale biocompatible soft robots can be envisioned to perform complex autonomous tasks in the human body and microfluidic systems such as cargo transport and drug delivery.[44-48] As stimuli-responsive hydrogels become more important in biomedical and other applications, researchers seek to further understand the physics and dynamic behaviour of these smart materials in order to design more advanced functional devices.

To this end, a range of theoretical models has been developed over the years to characterize the behaviour of responsive hydrogels. These include not only models that predict equilibrium volume transitions,[49, 50] but also the swelling kinetics of responsive gels.[51-55] The models were successfully tested in recent experiments on the swelling kinetics and volume phase change in a variety of responsive hydrogel systems.[56-59] Theoretical models, however, inherit certain limitations that restrain their utility in practical engineering applications. The equilibrium phase transition models do not characterize the swelling kinetics of hydrogels, which is important for mechanical actuation devices and drug delivery vesicles. Simple linear models for swelling kinetics on the other hand are usually limited by small deformations, while

applicable for larger deformations nonlinear theories pose significant difficulties in their solution.[51]

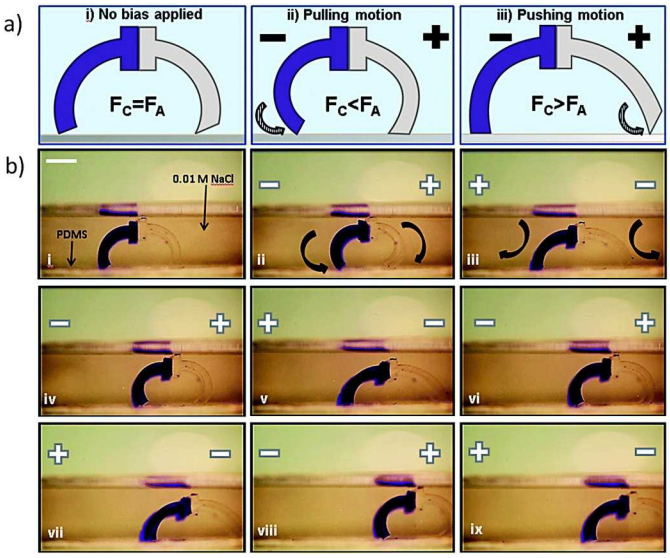

Fig. 1 An example of a synthetic responsive hydrogel walker and its actuation mechanism. (a) Depending on the direction of the applied electric field, the walker undergoes either a "pushing" or "pulling" mode of actuation. F_C and F_A represent the friction forces of the cationic leg (dark blue) and anionic leg (light grey), respectively. (b) The gel walker in motion in 0.01 M NaCl composed of 50% NaAc and 30% DMAEMA-Q legs with an applied electric field of 5 V/cm. Scale bar = 5 mm. Reproduced from ref. 23 with permission from The Royal Society of Chemistry.

The theoretical models typically do not explicitly capture the solvent hydrodynamics, which requires complex, long-range coupling between the polymer network and solvent. These limitations thus point to the need for general computational tools that can simulate the complex unsteady physics governing the swelling kinetics of responsive hydrogels with high fidelity. The rise of high performance computing has made numerical simulations of these responsive polymer networks more feasible. Recent computational studies of smart hydrogels offer insights that extend beyond validating theoretical models or reproducing experimental results. The wide parameter space available in a numerical simulation overcomes various limitations in the laboratory. For example, computational simulations are employed to simulate the drug delivery process inside the human body, which is an environment difficult to replicate in experiments.[60] This information can be used to design more effective or alternative drug delivery systems.[61-64] Furthermore, the design of soft robotics is facilitated using computational simulations, as all system parameters can be systematically probed and their effects established. In an experimental design such as of the aforementioned hydrogel walker,[23] the effect of walker geometry on the speed, for example, may be only determined through a series of elaborated experiments.

In this feature article, we discuss the recent progress in the computational modelling of stimuli-sensitive hydrogel networks. Our focus is on the emerging application of *mesoscale computational models*, specifically dissipative particle dynamics (DPD).[65] First, we present a brief overview of currently used computational models. Then we discuss specific approaches that were adapted for modelling responsive hydrogels. Finally, we describe recent studies that have used DPD to examine the properties of hydrogels and to probe their utility in functional stimuli-controlled systems. As mesoscale modelling of responsive hydrogels is relatively new, our goal is to elucidate exciting new research paths and bring awareness to the useful modelling techniques in designing functional small-scale devices comprising responsive hydrogels.

2. Overview of computational methods

Responsive hydrogels are complex systems involving phenomena that occur at length and time scales ranging from those that represent the dynamics of a single polymer chain to the scales that characterize the kinetics of the bulk hydrogel material. Thus, a wide variety of computational models, ranging in spatial and time scales from atomistic simulation methods to full continuum models, have been developed and employed to examine the behaviour of these multicomponent polymer systems.

2.1 Atomistic models

Atomistic models such as molecular dynamics (MD) and Monte-Carlo (MC) methods are used to accurately resolve the atom-level behaviour of polymer systems. In a fully atomistic simulation, MD directly solves for the motion for all atoms and molecules. Here, single particles represent atoms that interact via relevant attractive and repulsive potentials. The particle positions are integrated in time based on the forces derived from the potentials. Thus, MD simulations can directly capture the molecular-level dynamics of polymeric materials at atomistic scales. For example, recent atomistic MD studies have been performed on material properties of different kinds of cross-linked polymer networks[66-68] and the behaviour of responsive hydrogels.[69, 70] These atomistic scale simulations come with a highly expensive computational cost, however. Because of the sheer number of molecules composing hydrogels and associated computational time, fully atomistic MD simulations are limited to simulating polymer systems at small scales and cannot reproduce the large-scale macroscopic behaviour.

To simulate larger spatial and time scales, coarse graining is employed.[71] In a coarse grained MD simulation, multiple atoms are represented by a single particle. Effective interactions between these particles represent the collective motion of the groups of atoms. Coarse grained simulations are typically mapped from smaller scale atomistic simulations.[72] For example, as shown in Fig. 2, a coarse-grained MD to atomistic MD mapping and reverse mapping procedure was developed in order to study the material properties of a hypercross-linked polystyrene network.

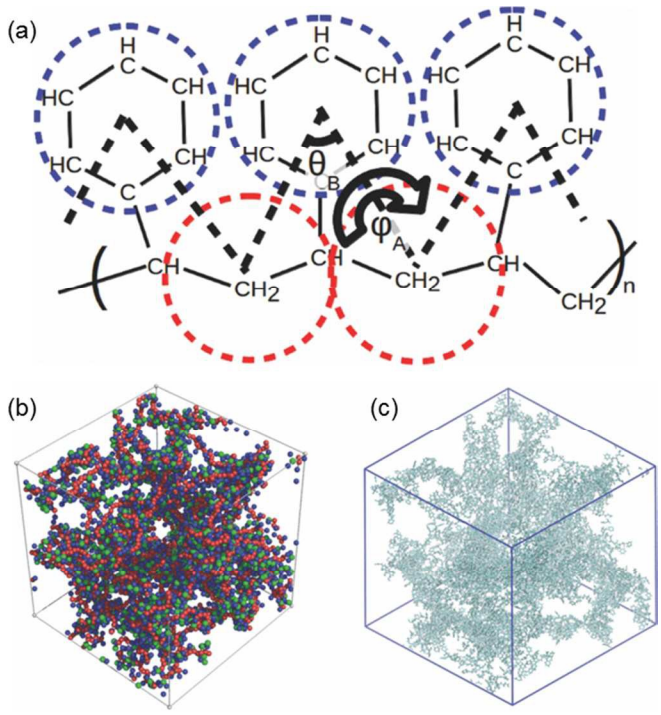

Fig. 2 (a) Example of a coarse graining mapping procedure. Bead A (red) represents the centre of mass of the CH2 group and the two neighbouring CH groups. Bead B (blue) represents the phenyl group. (b) Coarse-grained representation in simulation cell with corresponding reverse mapped atomistic presentation in (c). Their coarse-grained model allowed for simulations at larger time and spatial scales in order to reduce number of calculations and achieve results in reasonable time. Reprinted with permission from ref 72. Copyright 2014, AIP Publishing LLC.

Coarse-grained potentials are typically softer than the atomistic potentials.[71] Thus, coarse-graining not only drastically reduces the number of particles used in simulations, but also allows for larger integration time steps, which in turn enable the simulation of the polymer systems with larger time and length scales. This makes coarse grained molecular dynamics simulations an attractive tool for studying dynamic polymeric systems such as responsive polymer brushes[73, 74] and hydrogels[75-79] at scales larger (by approximately ten times)[71] than fully atomistic simulations.

Monte Carlo methods have been used to model equilibrium states of polymer systems.[80-82] All molecules have specific degrees of freedom in space. In MC simulations, small random changes are made to the molecular configurations. The new configuration is accepted if the energy change is within a prescribed criterion based on probability. Thus, the method produces a sequence of configurations that lead to specific equilibrium states. Though the methods are computationally much cheaper compared to MD, MC may not necessarily capture the kinetics correctly because the evolution in time is not explicitly modelled.

2.2 Continuum models

The macroscale behaviour of stimuli-responsive hydrogels was studied using scaling theories[83-86] and models that are based on continuum mechanics of the polymer networks and solvent,[52, 53, 87-91] which are typically solved numerically. An interesting recent example is shown in Fig. 3, where a finite element model (FEM) was employed to investigate the self-folding of combined responsive and non-responsive gel layers.[92] Here, the thermoresponsive gel PNIPAM (shown in green) swells in volume with decreasing temperature. The swelling causes bending in the passive layers, ultimately leading to a closed box as shown in Fig. 3d.

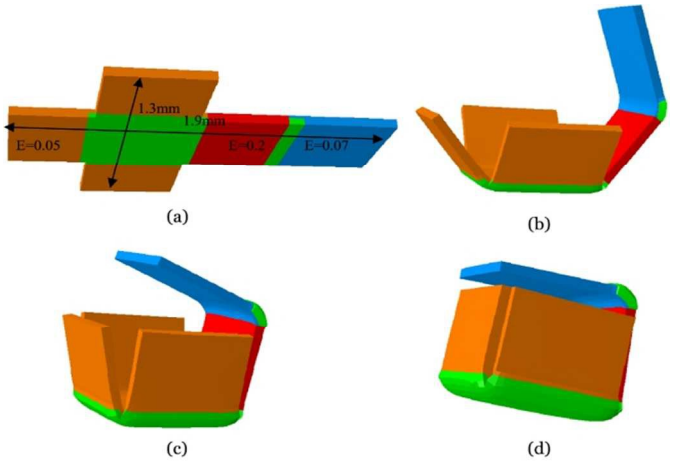

Fig. 3 FEM model of a self-folding box using multiple responsive and non-responsive gel layers. (a) Original 2D configuration at T = 300 K. Green surface is the temperature responsive layer, while other colours represent passive layers with different moduli as labelled. (b) and (c) represent intermediate stages of the folding process at T = 290 K and T = 280 K, respectively. The responsive layer expands in volume as the temperature decreases (d) shows the final closed box at T = 273 K. Reproduced from ref. 92 by permission of IOP Publishing. Copyright 2013 IOP Publishing. All rights reserved.

In contrast to atomistic models, macroscale models can simulate responsive gel swelling kinetics at large time and spatial scales but cannot capture atomistic scale effects. Macroscale models are based on transport equations and derived from conservation laws and constitutive relations.[93] Mass conservation leads to differential transport equations describing the time evolution of concentrations of all chemical species. Furthermore, momentum conservation yields an equation describing the gel deformation and velocity field. These equations require a number of material constitutive relationships that must be known or determined *a priori*. For polyelectrolyte gels, which expand in volume under applied electric fields, Maxwell's equations need to be incorporated into the model to describe the electric field evolution.[93, 94]

If the swelling deformations are small, a linear stress-strain relationship in the gel can be used and the gel-solvent interface can be assumed to be stationary.[93] On the other hand, large gel swelling deformations require nonlinear finite displacement theories.[95, 96] If the solvent is modelled as a separate domain, interface tracking schemes, such as phase field models, can be used to fully capture the kinetics of large deformations.[97, 98] In this case, a separate transport equation must be derived to describe the evolution of the phase field variable. The set of

fully coupled transport equations with appropriate boundary conditions is then solved numerically using finite difference[97] or finite element methods.[99]

2.3 Mesoscale models

Atomistic models are limited by the small spatial and time scales, while macroscale methods require constitutive relations which may not be known. Therefore, a need arises for an intermediate approach that circumvents these inherent difficulties. Mesoscale models provide a useful compromise.[100] Though these models do not simulate atomistic details, they reproduce the bulk properties and swelling kinetics without requiring complicated constitutive relationships. Because of these advantages, meshless and lattice-based mesoscale models of responsive polymer gels are gaining more widespread use.

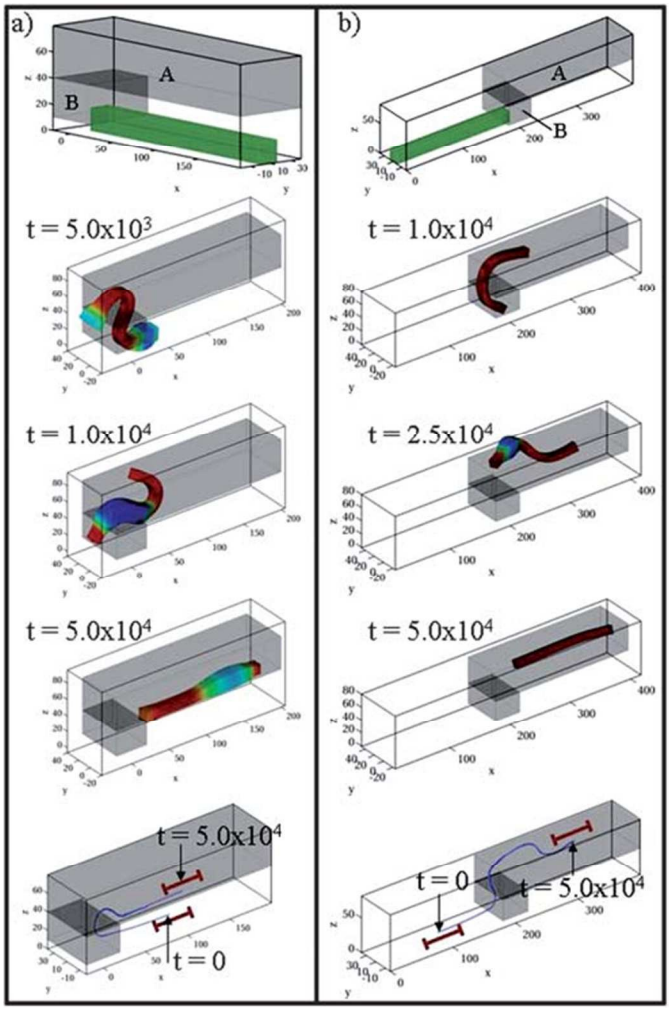

Fig. 4 Self-oscillating BZ gel walker. Depending on starting positions in (a) or (b), the gel walker follows different trajectories, but still finishes in the darker region A. The simulations demonstrate how the light intensity can be used to influence the motion of BZ gel walkers. Reproduced from ref. 101 with permission from The Royal Society of Chemistry.

Lattice based models are emerging approaches for simulation of hydrogels. A lattice spring method (LSM) discretizes an elastic material into a lattice network of masses and harmonic springs.[102, 103] Traditionally, the method was applied to continuous solids but can approximate the structure of polymers and responsive gels.[104, 105]

A gel lattice spring method (gLSM)[106] was developed to model self-oscillating hydrogels undergoing the Belousov-Zhabotinsky reaction, or BZ gels.[107] Unlike traditional stimuli-responsive gels, BZ gels undergo continuous periodic swelling and de-swelling due to an ongoing chemical reaction.[108-111] In gLSM, the domain is discretized into a lattice network of mass nodes. Nodes experience forces due to the rubber elasticity of the cross-linked polymer network and from the internal pressure (this includes the Flory-Huggins osmotic pressure due to polymer-solvent coupling). Equations that describe the BZ reaction kinetics are coupled to the gel kinetics resulting in periodic deformation waves propagating through the gel network.[112] Using gLSM, researchers have designed a self-propelling hydrogel "walker" that can move using a stiffness gradient in the gel.[101, 113] Furthermore, the photosensitivity of BZ gels allows the walker to be directed by light and made to follow different paths. Specifically, as shown in Fig. 4, the walker is directed into the darker A and B regions. Depending on either initial condition of Fig. 4a or Fig. 4b, the walker takes different trajectories but ultimately settles into the darker A region. Thus, these simulations show how light intensity can be used to direct the motion of BZ gel walkers.

The dynamics of hydrogels immersed in solvents can be strongly affected by the emerging fluid flows. The lattice Boltzmann method (LBM) can be used to model the solvent hydrodynamics.[114-117] Unlike traditional continuum methods that directly solve the Navier-Stokes equations, LBM solves the discrete Boltzmann equation. In LBM, the fluid domain is discretized into a set of lattice nodes, and the solvent is characterized by a velocity distribution function. Hydrodynamic quantities are then calculated as moments of the velocity distribution function. An approach that integrates LBM with LSM[118-120] has been used to design a responsive hydrogel swimmer that can self-propel in a highly viscous environment using a series of flaps (Fig. 5).[104] Here, a periodic external stimulus is applied to the gel swimmer body, which causes the propulsive flaps to oscillate in a time irreversible manner. Fig. 5 shows snapshots of the time history of the swimming stroke.

Other techniques used for mesoscale hydrogel modelling include meshless particle based methods such as Brownian dynamics (BD)[121] and dissipative particle dynamics (DPD).[65] The mesh-free approach allows one to avoid the difficult interface reconstruction and tracking problems that arise in continuum methods. In Brownian dynamics particles are assumed to have no inertia but evolve in time in response to an interaction potential and a random Gaussian-distributed force to mimic thermal fluctuations.[122] A friction force mimics the solvent interaction and the solvent kinetics is normally not explicitly included to reduce the simulation time. This is useful if there is a large time scale separation between the polymer and solvent dynamics.[123] Brownian dynamics is typically used with coarse-grained polymeric models and has been used to study entangled polymeric liquids,[124] diffusion of solutes in

hydrogels,[125, 126] and rheology of polymers.[127, 128] BD has also been incorporated into the LBM model directly[129] or with the addition of a fluctuating term in the collision operator.[130] The latter has been used to simulate kinetics of polymer solutions.[131]

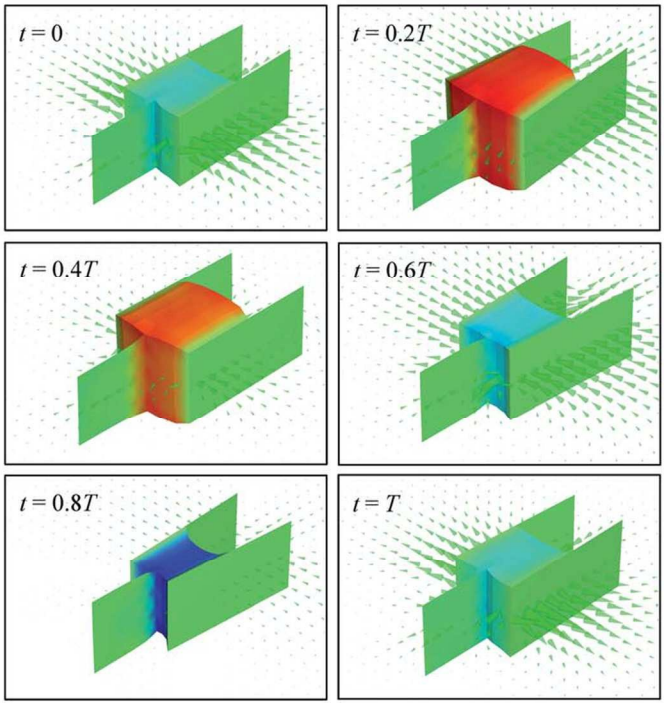

Fig. 5 Responsive gel swimmer design with attached flaps. The swimmer kinetics was modelled using a coupled LBM-LSM approach. The hydrogel expands and contracts in response to a periodic external stimulus. Here, pictures show the swimming stroke at various points during the period. Adapted from Ref. 104 with permission from The Royal Society of Chemistry.

Finally, dissipative particle dynamics (DPD) is a powerful mesoscale approach developed in recent decades.[65, 132-136] Similar to coarse-grained molecular dynamics, clusters of molecules are represented by DPD particles interacting through soft potentials within a cut-off radius, allowing simulation of larger time and spatial scales. DPD particles also experience dissipative forces that lead to viscosity and stochastic forces that account for thermal fluctuations. The dissipative and stochastic forces are related through fluctuation-dissipation theorem and constitute a DPD thermostat that keeps the system in thermal equilibrium.[137] In contrast to MD, all interactions in DPD are pairwise, conserving momentum exactly. This leads to accurate modelling of hydrodynamic effects even with a relatively small number of particles.[138] Furthermore, different coarse-graining procedures can be employed to map DPD potential to MD results.[139, 140] The dynamics of DPD system is simulated by integrating Newton's law in time for all DPD beads, usually using the velocity Verlet algorithm.[141, 142] Thus, DPD is a mesoscale method that can capture the coupled kinetics of polymer networks and the solvent.

3. Mesoscale modelling of hydrogels

Hydrogels are networks composed of chemically or physically cross-linked polymer chains immersed into a solvent. Thus, hydrogel modelling requires a mesoscale model of a polymer network that both reproduces relevant material characteristics and properly describes interactions with the solvent. In turn, a mesoscale model is required for the polymer chains that constitute the network.

3.1 Polymer chain models

A detailed model of a polymer chain using atomistic MD may include all of the individual atoms and bond interactions. In mesoscale models, the polymer chain is coarse-grained. A common approach is to approximate the polymer chain using the bead-spring model.[143] In this approach, a single polymer chain is represented by a series of beads connected in a chain that interact through bending, stretching, and torsional potentials. These spring potentials are typically set to reproduce the bulk behaviour of the polymer chains, whereas the exact form of the potentials varies among different models.

The simplest interaction potential between beads within the chain is the simple harmonic potential (Rouse model). This model requires a separate repulsive force, as included in DPD, to maintain a nonzero equilibrium distance between beads. Furthermore, this soft potential does not limit the separation distance between beads. When the model is coupled with DPD, this can lead to undesirable behaviour, such as chain crossing, if the beads are stretched too far.[144] In order to reduce these unphysical effects, Fraenkel springs may be used.[145] Additionally, the beads can interact via a harmonic bending potential. The combination of harmonic spring and bending potentials leads to a simple elastic model of a polymer chain.[62, 146, 147]

Non-linear potentials have also been considered. One common potential was developed by Kremer and Grest, some of the first researchers to use computer simulations to model polymer chains.[148-150] The Kremer-Grest polymer chain consists of beads that are connected linearly and interact via a pairwise potential. The potential is divided up into two parts: a Lennard-Jones potential that accounts for excluded volume and a strong attractive potential to maintain the bound topology. The choice of the strong attractive potential varies among different models, but typically is given by the finitely extensible nonlinear elastic (FENE) potential. This model polymer chain has been used in many recent studies of the mechanical properties entangled polymer networks.[75, 151, 152] Other non-linear bead-spring potentials include the general COMPASS potential,[153] worm-like chain (WLC) potentials (widely used for DNA simulations),[154-156] inverse Langevin potentials,[154, 157] and others.[158] More details behind the relevance, usage, and limitations of these different models can be found elsewhere.[159]

3.2 Hydrogel network models

Hydrogel networks contain cross-links that prevent dissolution into the surrounding solvent. Cross-links may be chemically or physically induced by a variety of experimental means.[160]

Chemical cross-links are composed of chemical bonds created through radical polymerization reactions while physical cross-links stem from physical interactions such as entanglements or ionic interactions. The randomly distributed nature of gel networks with cross-links poses certain technical challenges in computational modelling. The hydrogel network model should accurately reproduce not only the relevant material properties like strain response of an actual hydrogel, but also physical characteristics like porosity, connectivity, and cross-link density. Model networks thus are created using several different approaches. An example of a three-dimensional model network[161] is shown in Fig. 6. Here, Fig. 6a shows the cross-linked network in the computational domain, while Fig. 6b zooms in to part of the network to highlight the connecting cross-links with the number of connections labelled.

A common approach is to mimic an actual polymerization reaction in which cross-linking agents are added to a mixture of monomers. These reactants undergo polymerization to form a gel network. To simulate this process, polymer chains are randomly distributed within the computational domain. This step is straightforward to implement and the average chain length can be readily imposed. However, creating cross-links is not as trivial. One solution is to evolve the filaments over time, creating cross-links when filaments intersect[162] or approach each other within a specified cut-off distance.[161, 163] The entire process is continued until the desired mean cross-link spacing is achieved. Thus, the topological characteristics of the network can be controlled. Another cross-linking procedure is to simulate the chemical reactions and subsequent bonds using a Monte Carlo method.[164, 165]

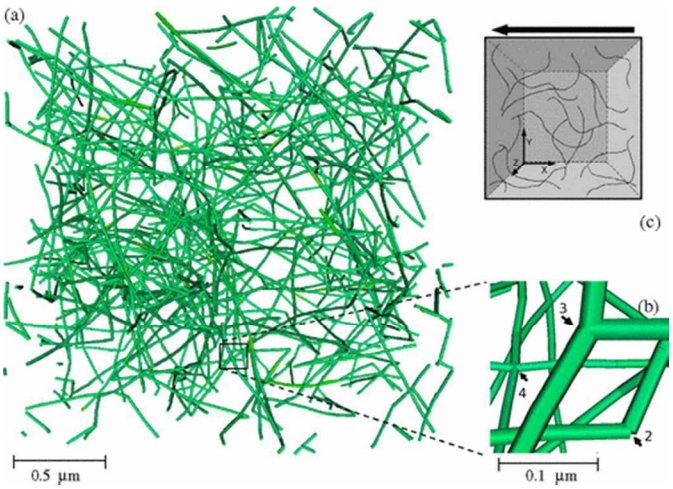

Fig. 6 (a) Three-dimensional cross-linked polymer network model. (b) Zoomed in part of (a) that shows cross-link with 2, 3, and 4 connections. (c) Schematic of simulation box with network inside. Reprinted figure with permission from ref. 161. Copyright 2007 by the American Physical Society.

The cross-linking procedure is not limited to coarse-grained simulations. The polymerization reaction can be modelled using MD simulations. Starting with a mixture of monomers and cross-linker molecules, MD simulations are performed to equilibrate the system and form appropriate cross-linking chemical bonds. The resulting network topology is examined and then coarse-grained for use in mesoscale simulations.[166, 167] Despite the larger number of steps and thus longer computation time, this approach is useful for accurately modelling the behaviour of specifically known polymer network systems.

To avoid the complications of simulating either a specific or general polymerization reaction, an alternative approach has been developed.[147, 168-171] In this model, the cross-link nodes, not the filaments, are first randomly distributed in the domain. Then the cross-linked nodes are connected using filaments to a specified number of neighbouring nodes, controlling the average connectivity and cross-link density of the network. The method has the advantage of an explicit control over the network topology including creating networks with pre-described non-uniform distributions of network parameters. Furthermore, this approach decreases computation times to initialize a polymer network. While this approach can only yield a general polymer network model, these models can be matched to physical polymer networks by examining the system response and appropriately tuning model parameters.

We note that the aforementioned polymer network models are more suitable for modelling chemically and physically cross-linked networks with fixed topology since the cross-linked points form a part of the internal structure. However, physically cross-linked networks that experience sufficiently large stresses may break apart at cross-linked points and drastically change the network topology. The repeated rupture and formation of physical cross-links under shear lead to viscoelastic flow behaviour compared to a more solid-like behaviour of chemically cross-linked gels.[172-174] Furthermore, the shear viscosity of physically cross-linked gels has been found to decrease with the rupture rate of cross-links.[172] In modelling, physically cross-linked networks must be constructed indirectly by equilibrating a solution of polymer chains and modelling the relevant physical mechanisms causing cross-linking (such as amphiphilic ends or entanglements).[175-179]

Once the polymer network is initialized, the hydrogel model is completed when the network is immersed in a solvent. The solvent is modelled in DPD by randomly distributed beads that interact with the polymer networks via the DPD potentials. In this case, the filaments are characterized by specific values of Stokes-Einstein radius.[180] The magnitude of the repulsion potential between the polymer and solvent beads accounts for the network hydrophobicity. It can be tuned to represent a particular value for the Flory-Huggins interaction parameter.[181]

3.3 Hydrogel kinetics model

Hydrogels can respond by swelling and de-swelling to changes in the environment. Specifically, the environmental changes can increase osmotic pressure inside the gel, causing it to expand outward and allow solvent to diffuse inward. For example, poly (N-isopropylacrylamide) (PNIPAM), is a well-studied temperature responsive polymer that undergoes a volumetric phase change past its lower critical solution

temperature (LCST).[182] Below the LCST, the hydrogel exhibits hydrophilic properties and is miscible in water, allowing water molecules to enter the gel and increasing the gel volume. Above the LCST, however, PNIPAM undergoes a conformal change, lowering its volume and forcing more water molecules out, behaving in a hydrophobic-like manner.[183] The equilibrium states are illustrated in Fig. 7 for a recently fabricated nano-structured hydrogel (NSG).[184] Here, the NSG is composed of smaller active nanogels (green spheres) that act as cross-linkers bridged by NIPAM strands. The NSGs were found to exhibit higher volume ratios as well as more rapid swelling (Fig. 7d). Another specific swelling mechanism involves polyelectrolyte gels responding to changes in pH. Here, the pH change induces a flow of ions into the gel, increasing the osmotic pressure, which leads to gel expansion.[185]

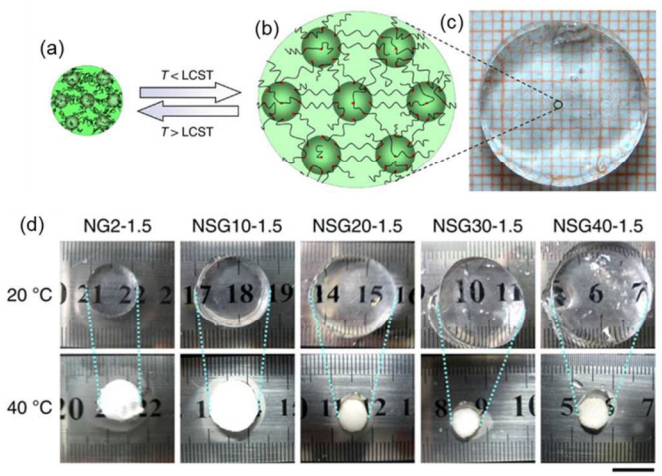

Fig. 7 Nano-structured hydrogel with active nanogel cross-linkers bridged with NIPAM strands. (a) and (b) illustrate the swelling and de-swelling process based on whether temperature is lower or higher than LCST. (c) Optical image of swollen NSG. (d) Comparison of equilibrium states of NSGs with regular PNIPAM hydrogel (denoted as NG). The numbers after NSG indicate the polymerization time of cross-linker nanogels. NSGs show improved swelling ratio for all cases. Scale bar indicates 1 cm. Adapted from Ref. 184 under the Creative Commons Attribution 3.0 Unported License.

The swelling kinetics can be captured directly using atomistic MD[186] or by solving transport equations in continuum methods.[187] In DPD, the kinetics of a swelling and contracting responsive hydrogel due to an external stimulus can be modelled by changing the interactions of the network filaments with the solvent[188] and/or by changing the filament equilibrium length. The latter can be achieved by adjusting the DPD repulsion strength between DPD particles constituting filaments[189] and/or the equilibrium length of the polymer chain model (for example, the equilibrium length of a Fraenkel spring).[62] Physically, altering the repulsion strength changes the osmotic pressure, resulting in a new equilibrium gel size when the system equilibrates. The stimulus strength can also be varied in time, simulating a time dependent response of the hydrogel in the evolving environment.

After the network is changed to mimic the application of a stimulus, the gel gradually relaxes to its new equilibrium state. In the overdamped system, the equilibration process is defined by a balance between forces associated with the change of the gel free energy and viscous drag due to the solvent penetrating into the gel network. It is therefore important that the gel model can properly capture both the network elasticity and interactions with the viscous solvent to correctly reproduce gel swelling kinetics. In practice, collective diffusion can be used to compare the model network with experimental gels.[55]

In the spatial domain, the DPD simulations are scaled to the physical system via the cut-off radius of the conservative potential.[190] At small scales, the coarse-grained nature of DPD may not correctly capture the behaviour of individual polymer strands, but this is not an issue if the bulk behaviour of the network is examined (in for example, drug delivery applications using nanogels). Indeed, DPD has been used to simulate physical systems on the nanoscale with cut-off radii on the order of single nanometers.[61, 190] On large scales, DPD is limited by compressibility effects and diffusion time scales, although modifications have been proposed for simulation of fluid flows with Reynolds numbers as high as 1000.[191] Thus, DPD is applicable to a wide range of length scales from nanogels to centimetre sized gels, making the method useful for a large variety of applications.

4. Applications of mesoscale modelling

In this section we describe several recent examples in which DPD was used to investigate hydrogel properties and to probe the utility of hydrogels in practical engineering applications. As an exciting, emerging field, there are relatively few studies in this area. Thus we discuss examples from the current literature that motivate possible future research paths.

4.1 Mechanical and transport properties

Hydrogels can undergo large elastic deformations leading to complex nonlinear viscoelastic behaviour.[192] Depending on loading conditions, the material and transport properties can be anisotropic. In this respect, mesoscale models have been used to perform structural analyses on hydrogels in order to determine material coefficients and design high performance gels.

Recent research has focused on the material properties of amphiphilic copolymers, which are polymer chains comprising two or more different types of monomers. To be amphiphilic, some monomers must be solvent selective and others solvent incompatible. These amphiphilic copolymers have been shown to undergo sol-gel transition at a critical polymer concentration and self-assemble into complicated physically cross-linked gel networks.[177, 193]

Several studies have used mesoscale modelling to study the material properties of physically cross-linked amphiphilic copolymer hydrogels. In particular, the morphological and material properties of self-assembled ABA triblock copolymers was examined using DPD.[178] The study used a bead-spring model with a FENE potential to model the triblock polymer chain and found that the solvent-incompatible A-blocks self-

assemble into micelles connected by B-block bridges and loops. The elastic modulus of the network structure was estimated by monitoring the response to an oscillatory external force. This model, however, suffered from the problem of chain crossing, underestimating the elastic modulus.

To account for excluded volume and entanglements, a modified segmental repulsive potential (mSRP) was introduced.[194] This model added bond-bond repulsion while preserving the thermodynamics of standard DPD and was used to study the morphological and mechanical properties of ABA triblock copolymers.[175] It was found that the micelle size increased nearly linearly with polymer concentration. Also, the separate contributions of cross-linking and entanglements to the elastic modulus each were determined by fitting to a constitutive relation.

The material properties of amphiphilic graft copolymers were also studied. In contrast to block copolymers, which have blocks arranged linearly, graft copolymers have a backbone polymer chain with several polymeric branches. Using DPD, researchers showed that ABC amphiphilic graft copolymers (where A is the solvophilic backbone) also self-assemble into physically cross-linked gel networks and exhibit high structural performance.[176] As shown in Fig. 8, the extensional modulus increases greatly with polymer concentration. At lower concentrations, ABC graft copolymers exhibit a micelle solution with low modulus. At higher concentrations, the graft copolymers form physically cross-linked gels that exhibit stiffer behaviour. At all concentrations the ABC graft copolymer is found to have a larger modulus than both AB graft copolymers and BAC triblock copolymers.

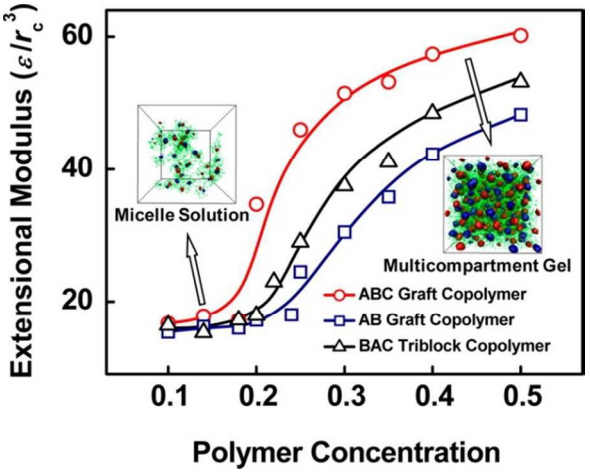

Fig. 8 Elastic properties of ABC amphiphilic graft copolymers as studied using DPD. ABC graft copolymers exhibit higher extensional moduli than both AB graft copolymers and BAC triblock copolymers. At high polymer concentrations, the ABC graft copolymers form physically cross-linked gels. Reprinted with permission from ref. 176. Copyright 2013 American Chemical Society.

In addition to mechanical properties of hydrogels, transport properties are also necessary to design functional hydrogel systems especially for drug delivery applications. The permeability and diffusion through a random polymer network were studied using DPD.[147] Here, a cross-linked network model was developed and the unstressed isotropic permeability and diffusion were measured and found good agreement with experimental data. The anisotropic transport properties under both normal and shear deformations were examined and showed to depend on the local filament orientation. Further understanding mechanical and transport properties of hydrogels in different dynamic conditions can lead to optimized synthetic hydrogel systems for applications like soft robotics and drug delivery.

4.2 Self-propelling soft robots

Responsive hydrogels under an applied stimulus can undergo large macroscale deformations, naturally making such materials suitable for actuation in a variety of soft robotic systems. Many computational designs for actuators and propulsors such as a the aforementioned BZ gel walker[101, 113] exist at the millimetre scales and larger where continuum methods are more widely used.[93] However, locomotion at the micron and sub-micron scales is nontrivial and requires biomimetic approaches for propulsion such as biocatalytic propulsors[195] and synthetic beating nanowires.[196] Responsive hydrogels also have the potential to be useful as efficient microscale actuators and propulsors since they can be controlled directly by the environment without the need for complex mechanical parts. Furthermore, they can exhibit fast response times at small scales.[197, 198]

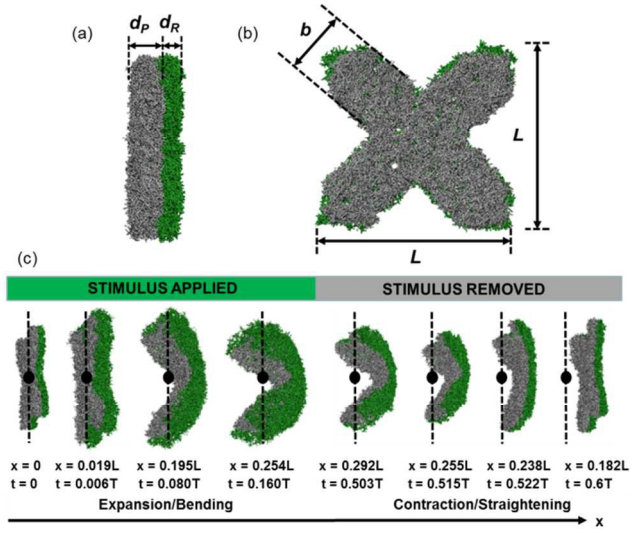

Fig. 9 A microswimmer composed of a bilayered hydrogel. (a) Side view and (b) top view of the microswimmer. The green layer is responsive and swells when external stimulus is applied, while the grey layer is passive. (c) Swimming stroke and resulting displacement during one period while an external stimulus is applied and removed. Adapted with permission from ref. 199. Copyright 2014 American Chemical Society.

Indeed, the use of responsive hydrogels for designing self-propelling robots has recently been demonstrated in the micron scale using DPD simulations.[199] In this study a bilayered hydrogel microscopic robotic swimmer was designed and shown to propel forward successfully in a viscous solvent. The microswimmer was composed of two bonded layers, one of

which is responsive to an external stimulus and the other is passive (Fig. 9a,b). The study found that the gel swimmer deformed periodically under the influence of a periodic external stimulus. Specifically, the swimmer undergoes a sequence of four steps: expansion, bending, contraction, and straightening, leading to a time irreversible motion required for propulsion through a highly viscous solvent (Fig. 9c). It is expected that such robotic swimmers can be employed to pick-up and transport cargoes to a specific locations in microscale systems. The design of such systems will directly benefit from the use of mesoscale modelling approaches such as DPD.

4.3 Drug delivery systems

Hydrogels are typically biocompatible, making them attractive materials for synthetic drug delivery systems. In such systems, the drug particles can be encapsulated within a responsive gel network. Controlled release and storage of the drug particles can be achieved by triggering an external stimulus to collapse the encapsulation structure. For example, a common design for cancer drug dispersion uses pH responsive polymeric materials, as the external environment around cancer cells typically has a lower pH.[200] As experimental investigations of drug delivery designs are difficult to perform, mesoscale numerical simulations provide a valuable practical means to study new drug delivery mechanisms.

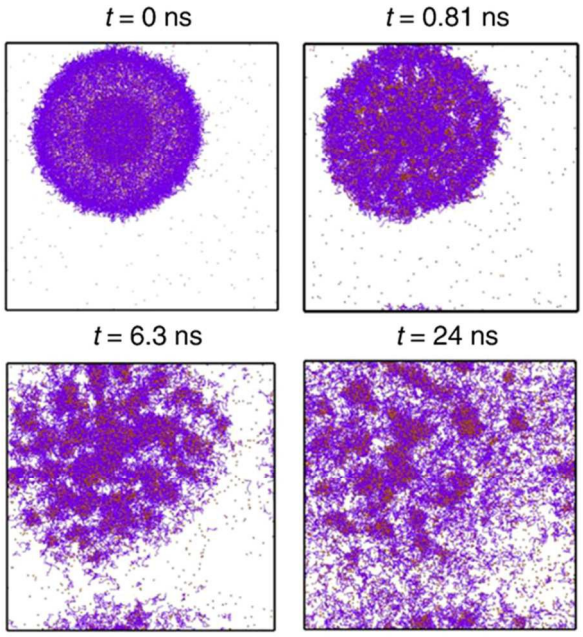

Fig. 10 A pH-responsive hydrogel-like micelle encapsulation composed of PAE-PEG amphiphilic copolymers as studied using a combination of MD and DPD. PEG is shown as purple and the drug CPT is shown in orange. The snapshots illustrate the drug release process when the pH is reduced. Reprinted from ref. 63, Copyright 2012, with permission from Elsevier.

Several recent DPD studies on drug delivery designs focus on the self-assembly of amphiphilic copolymers to form hydrogel-like micelle structures. One such study used DPD to simulate the release of drugs from a pH-responsive micelle encapsulation.[64] Cracks were generated in the micelle when the pH was reduced, allowing for the controlled release of the interior drug particles. Another study investigated the storage and release of drug particles within PAE-PEG copolymer micelles.[63] Using a combination of MD and DPD, the simulations showed that an initially random configuration of copolymers and drug particles would equilibrate into micelles, containing the drug. When the pH was reduced, the micelles break apart, releasing the stored drug (Fig. 10). These studies illustrate potential drug delivery mechanisms using pH responsive hydrogel-like polymeric micelles.

Besides self-assembled co-polymer micelles, hollow stimuli-responsive hydrogel shells can also be used as drug delivery vesicles.[201-203] The controlled release of nanoparticles and macromolecules encapsulated within a responsive hydrogel microcapsule was studied using DPD (Fig. 11).[62] Such a system mimics a drug carrier in which the drug is initially stored in the interior of a hollow gel microcapsule. The study found that capsule swelling increases pore size and enhances diffusion of encapsulated solutes (Fig. 11a,b), whereas de-swelling leads to a squeezing effect that releases solutes rapidly (Fig. 11c). In the latter case, microscopic rods that stretch the capsule membrane can be added to regulate the release during capsule de-swelling (Fig. 11d). Furthermore, it was demonstrated that a periodically applied stimulus leads to pulsatile release of encapsulated solutes.

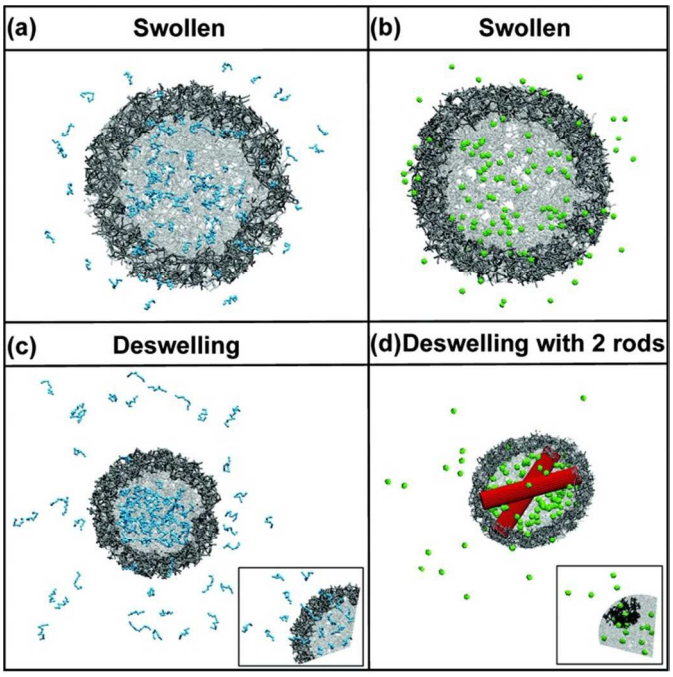

Fig. 11 DPD simulations of a hollow microgel capsule swelling and de-swelling under the influence of a periodic external stimulus. In the swollen state, (a) polymer chains (cyan) and (b) nanoparticles are released due to diffusion. When the gel contracts (c), the polymer chains are released more quickly due to a squeezing effect. (d) Microrods increase pore size and allow for a faster release of nanoparticles. Reprinted with permission from ref. 62. Copyright 2011 American Chemical Society.

4.4 Synthetic healing and tissue regeneration

Hydrogels have biocompatible physical characteristics and are appealing materials for use in tissue engineering and regenerative medicine applications.[204-206] Specifically, the hydrogel material properties can be tailored to resemble that of natural tissue and promote cellular attachment. Thus, hydrogels can be used as scaffolds for tissue regeneration. Also, hydrogels have been demonstrated as effective barriers against thrombosis and restenosis, improving a patient's prognosis during healing.[207, 208] Developments in the mesoscale modelling of hydrogels can therefore promote advances in synthetic healing technology.

Motivated by applications in regenerative medicine, researchers have investigated the nanostructure and micelle formation of four-arm star poly(ethylene glycol-*co*-lactide)-acrylate (SPELA) macromonomers.[209] These macromonomers are used in a hydrogel precursor solution in which acrylate groups undergo a polymerization reaction to form a robust hydrogel network. Lactide segments are added to introduce degradability to the hydrogels, but this causes unwanted micellization which traps acrylate groups, reducing the hydrogel strength. The DPD study identified the critical lactide length that leads to micellization. Furthermore, the study demonstrated a trade-off between hydrogel degradability and extensional modulus favouring degradability with increasing lactide segment length. An optimal lactide segment length could thus be chosen to design robust hydrogel networks as carriers for stem cell delivery in regenerative medicine.

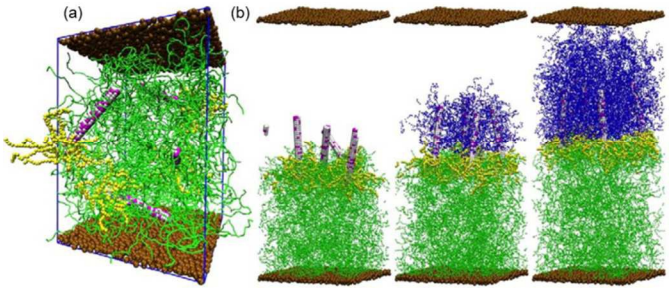

Fig. 12 DPD study of a self-regenerating composite gel material. (a) Equilibrium state of the polymer gel with embedded nanorods. Polymer strands are shown in green, while amorphous solid walls are shown in brown. (b) When the gel is severed, nanorods diffuse to the outer surface and initiate regeneration, forming a new gel (shown in blue). Reprinted with permission from ref. 146. Copyright 2013 American Chemical Society.

DPD was also used to design a nanocomposite gel material that can self-regenerate with the aid of embedded nanorods (Fig. 12).[146] Here, a model was developed for thermo-responsive hydrogels that accurately reproduced the continuous volume phase transition behaviour. To achieve this, the repulsion parameter was dynamically updated between the DPD polymer and solvent beads every 100 time steps as a function of the average polymer concentration within that time span. The polymerization reaction is initialized at the nanorods on the new severed interface and propagates until a new polymer network is formed (Fig. 12b). This synthetic gel layer regrowth study can lead to designing materials that are self-replenishing, extending their lifetime and functionality.

Finally, a recent experimental study has synthesized microgels that behave like platelets.[210] These platelet-like particles (PLPs) have been demonstrated to collapse a fibrin network, similar to the process in blood clotting. A simulation using DPD was developed to understand the physics of this process. The fibrin network was modelled as a random polymer network with uniformly distributed sticky PLPs. The simulations showed that the PLPs indeed caused network collapse. Furthermore, softer particles caused a greater degree of network collapse than stiffer ones. This study is important for development of synthetic wound management treatments that could dramatically increase healing time.

5. Summary and outlook

Stimuli-responsive hydrogels are polymer networks that exhibit a volume change in the presence of a specific external stimulus. The ability of these materials to convert chemical energy into mechanical work makes them especially attractive for designing small scale functional devices. While there have been extensive experimental and theoretical investigations of responsive hydrogels, computational models are still developing. These computational models can be used to study the complex interactions characterizing the gel swelling process. These methods range from atomistic scale MD models to macroscale continuum methods. Atomistic models, while accurate at very small time and length scales, are extremely computationally expensive. Continuum approaches are based on multiple transport equations, requiring relevant constitutive relationships, and result in an unwieldy set of coupled equations that are difficult to solve. Mesoscale modelling offers an impressive compromise. Mesoscale models are relatively simple to implement to capture essential hydrogel characteristics and processes while simulating time and length scales much larger than typical MD.

DPD is one of the more popular mesoscale methods that have been used to investigate hydrogels and their applications. The pairwise nature of the interactions in DPD leads to accurate simulations of hydrodynamic effects that are vital for modelling the swelling kinetics of polymer gels. In DPD, polymer chains are usually modelled as bead-spring filaments. The cross-linked gel network model can be generated using several different approaches. A common approach is to simulate the polymerization reaction to generate cross-links, connecting individual filaments to create chemically cross-linked networks. But the alternative approach is also employed in which the cross-linked points are first randomly distributed and then connected by polymer filaments. Swelling kinetics is modelled by altering filament properties and interactions.

DPD has been demonstrated as an effective tool in several recent fundamental and applied studies of hydrogels reviewed in this article including the understanding their material and transport properties, the use of hydrogels in soft robotics and drug delivery applications, and designing regenerative tissue. The large variety of applications points to the robustness of DPD and demonstrates how the emerging mesoscale method

can be used to guide the design of functional small-scale devices for engineering and biomedical applications. Development of such mesoscale modelling techniques creates exciting new research paths that will ultimately further our understanding of the complicated physics involved in responsive hydrogel systems and broaden their utility in practical engineering applications.

Acknowledgements

The authors acknowledge financial support from NSF CAREER award DMR-1255288. P.D.Y. thanks S. V. Nikolov for helpful and stimulating discussions.

References

[a] George W. Woodruff School of Mechanical Engineering, Georgia Institute of Technology. Email: alexander.alexeev@me.gatech.edu

1 Z. X. Zhang, K. L. Liu and J. Li, *Angew. Chem.*, 2013, **125**, 6300-6304.
2 H. S. Abandansari, E. Aghaghafari, M. R. Nabid and H. Niknejad, *Polymer*, 2013, **54**, 1329-1340.
3 A. Rotzetter, C. Schumacher, S. Bubenhofer, R. Grass, L. Gerber, M. Zeltner and W. Stark, *Adv. Mater.*, 2012, **24**, 5352-5356.
4 A. Nakagawa, F. Steiniger, W. Richter, A. Koschella, T. Heinze and H. Kamitakahara, *Langmuir*, 2012, **28**, 12609-12618.
5 G. Stoychev, N. Puretskiy and L. Ionov, *Soft Matter*, 2011, **7**, 3277-3279.
6 I. W. Hamley, G. Cheng and V. Castelletto, *Macromol. Biosci.*, 2011, **11**, 1068-1078.
7 A. C. Lima, W. Song, B. Blanco-Fernandez, C. Alvarez-Lorenzo and J. F. Mano, *Pharm. Res.*, 2011, **28**, 1294-1305.
8 L. Klouda and A. G. Mikos, *Eur. J. Pharm. Biopharm.*, 2008, **68**, 34-45.
9 E. Mah and R. Ghosh, *Processes*, 2013, **1**, 238-262.
10 J. P. Best, M. P. Neubauer, S. Javed, H. H. Dam, A. Fery and F. Caruso, *Langmuir*, 2013, **29**, 9814-9823.
11 V. Gopishetty, I. Tokarev and S. Minko, *J. Mater. Chem.*, 2012, **22**, 19482-19487.
12 L. He, D. E. Fullenkamp, J. G. Rivera and P. B. Messersmith, *Chem. Commun.*, 2011, **47**, 7497-7499.
13 M.-T. Popescu, S. Mourtas, G. Pampalakis, S. G. Antimisiaris and C. Tsitsilianis, *Biomacromolecules*, 2011, **12**, 3023-3030.
14 L. D. Zarzar, P. Kim and J. Aizenberg, *Adv. Mater.*, 2011, **23**, 1442-1446.
15 L. T. De Haan, J. M. Verjans, D. J. Broer, C. W. Bastiaansen and A. P. Schenning, *J. Am. Chem. Soc.*, 2014, **136**, 10585-10588.
16 M. Dai, O. T. Picot, J. M. Verjans, L. T. De Haan, A. P. Schenning, T. Peijs and C. W. Bastiaansen, *ACS Appl. Mater. Interfaces*, 2013, **5**, 4945-4950.
17 L. Shen, J. Fu, K. Fu, C. Picart and J. Ji, *Langmuir*, 2010, **26**, 16634-16637.
18 Q. Yan, J. Hu, R. Zhou, Y. Ju, Y. Yin and J. Yuan, *Chem. Commun.*, 2012, **48**, 1913-1915.
19 J. He and Y. Zhao, *Dyes Pigm.*, 2011, **89**, 278-283.
20 J. Lai, X. Mu, Y. Xu, X. Wu, C. Wu, C. Li, J. Chen and Y. Zhao, *Chem. Commun.*, 2010, **46**, 7370-7372.
21 J. Ge, E. Neofytou, T. J. Cahill Iii, R. E. Beygui and R. N. Zare, *ACS Nano*, 2011, **6**, 227-233.
22 G. Filipcsei, J. Feher and M. ZríNyi, *J. Mol. Struct.*, 2000, **554**, 109-117.
23 D. Morales, E. Palleau, M. D. Dickey and O. D. Velev, *Soft Matter*, 2014, **10**, 1337-1348.
24 F. Carpi, R. Kornbluh, P. Sommer-Larsen and G. Alici, *Bioinspiration Biomimetics*, 2011, **6**, 045006.
25 O. Philippova, A. Barabanova, V. Molchanov and A. Khokhlov, *Eur. Polym. J.*, 2011, **47**, 542-559.
26 M. Zrinyi, *Colloid Polym. Sci.*, 2000, **278**, 98-103.
27 S.-K. Ahn, R. M. Kasi, S.-C. Kim, N. Sharma and Y. Zhou, *Soft Matter*, 2008, **4**, 1151-1157.
28 Y. Osada and J. P. Gong, *Prog. Polym. Sci.*, 1993, **18**, 187-226.
29 D. Roy, J. N. Cambre and B. S. Sumerlin, *Prog. Polym. Sci.*, 2010, **35**, 278-301.
30 L. Zhou, M. Chen, Y. Guan and Y. Zhang, *Polym. Chem.*, 2014, **5**, 7081-7089.
31 Z. Li, J. Shen, H. Ma, X. Lu, M. Shi, N. Li and M. Ye, *Soft Matter*, 2012, **8**, 3139-3145.
32 Z. Zhang, L. Chen, C. Zhao, Y. Bai, M. Deng, H. Shan, X. Zhuang, X. Chen and X. Jing, *Polymer*, 2011, **52**, 676-682.
33 M. a. C. Stuart, W. T. Huck, J. Genzer, M. Müller, C. Ober, M. Stamm, G. B. Sukhorukov, I. Szleifer, V. V. Tsukruk and M. Urban, *Nat. Mater.*, 2010, **9**, 101-113.
34 M. R. Islam, Y. Gao, X. Li and M. J. Serpe, *J. Mater. Chem. B*, 2014, **2**, 2444-2451.
35 M. Honda, K. Kataoka, T. Seki and Y. Takeoka, *Langmuir*, 2009, **25**, 8349-8356.
36 J. Hu and S. Liu, *Macromolecules*, 2010, **43**, 8315-8330.
37 P. Matricardi, C. Di Meo, T. Coviello, W. E. Hennink and F. Alhaique, *Adv. Drug Delivery Rev.*, 2013, **65**, 1172-1187.
38 R. Geryak and V. V. Tsukruk, *Soft Matter*, 2014, **10**, 1246-1263.
39 P. Calvert, *Adv. Mater.*, 2009, **21**, 743-756.
40 N. Smeets and T. Hoare, *J. Polym. Sci., Part A: Polym. Chem.*, 2013, **51**, 3027-3043.
41 A. S. Hoffman, *Adv. Drug Delivery Rev.*, 2013, **65**, 10-16.
42 J. Ramos, A. Imaz, J. Callejas-Fernández, L. Barbosa-Barros, J. Estelrich, M. Quesada-Pérez and J. Forcada, *Soft Matter*, 2011, **7**, 5067-5082.
43 A. S. Hoffman, *Adv. Drug Delivery Rev.*, 2002, **54**, 3-12.
44 D. B. Weibel, P. Garstecki, D. Ryan, W. R. Diluzio, M. Mayer, J. E. Seto and G. M. Whitesides, *Proc. Natl. Acad. Sci. U. S. A.*, 2005, **102**, 11963-11967.
45 S. J. Ebbens, G. A. Buxton, A. Alexeev, A. Sadeghi and J. R. Howse, *Soft Matter*, 2012, **8**, 3077-3082.
46 L. Zhang, T. Petit, Y. Lu, B. E. Kratochvil, K. E. Peyer, R. Pei, J. Lou and B. J. Nelson, *ACS Nano*, 2010, **4**, 6228-6234.
47 R. Verberg, A. T. Dale, P. Kumar, A. Alexeev and A. C. Balazs, *J. R. Soc. Interface*, 2007, **4**, 349-357.
48 I. Kosif, C. C. Chang, Y. Bai, A. E. Ribbe, A. C. Balazs and T. Emrick, *Adv. Mater. Interfaces*, 2014, **1**, 1400121.
49 M. Quesada-Pérez, J. A. Maroto-Centeno, J. Forcada and R. Hidalgo-Alvarez, *Soft Matter*, 2011, **7**, 10536-10547.

50 A. A. Polotsky, F. A. Plamper and O. V. Borisov, *Macromolecules*, 2013, **46**, 8702-8709.
51 N. Bouklas and R. Huang, *Soft Matter*, 2012, **8**, 8194-8203.
52 C. Wang, Y. Li and Z. Hu, *Macromolecules*, 1997, **30**, 4727-4732.
53 T. Tanaka and D. J. Fillmore, *J. Chem. Phys.*, 1979, **70**, 1214-1218.
54 J. P. Keener, S. Sircar and A. L. Fogelson, *SIAM J. Appl. Math.*, 2011, **71**, 854-875.
55 T. Tanaka, E. Sato, Y. Hirokawa, S. Hirotsu and J. Peetermans, *Phys. Rev. Lett.*, 1985, **55**, 2455-2458.
56 L. Ninni, V. Ermatchkov, H. Hasse and G. Maurer, *Fluid Phase Equilib.*, 2013, **337**, 137-149.
57 J. Walter, J. Sehrt, J. Vrabec and H. Hasse, *J. Phys. Chem. B*, 2012, **116**, 5251-5259.
58 H. Tajima, Y. Yoshida and K. Yamagiwa, *Polymer*, 2011, **52**, 732-738.
59 J. Yoon, S. Cai, Z. Suo and R. C. Hayward, *Soft Matter*, 2010, **6**, 6004-6012.
60 L. Huynh, C. Neale, R. Pomès and C. Allen, *Nanomedicine*, 2012, **8**, 20-36.
61 C. Soto-Figueroa and L. Vicente, *Soft Matter*, 2011, **7**, 8224-8230.
62 H. Masoud and A. Alexeev, *ACS Nano*, 2011, **6**, 212-219.
63 Z. Luo and J. Jiang, *J. Controlled Release*, 2012, **162**, 185-193.
64 S. Y. Nie, Y. Sun, W. J. Lin, W. S. Wu, X. D. Guo, Y. Qian and L. J. Zhang, *J. Phys. Chem. B*, 2013, **117**, 13688-13697.
65 R. D. Groot and P. B. Warren, *J. Chem. Phys.*, 1997, **107**, 4423-4435.
66 N. Nouri and S. Ziaei-Rad, *Macromolecules*, 2011, **44**, 5481-5489.
67 L.-H. Tam and D. Lau, *RSC Adv.*, 2014, **4**, 33074-33081.
68 C. Li, E. Coons and A. Strachan, *Acta Mech.*, 2014, **225**, 1187-1196.
69 S. Deshmukh, D. A. Mooney, T. Mcdermott, S. Kulkarni and J. D. Macelroy, *Soft Matter*, 2009, **5**, 1514-1521.
70 T.-Y. Sun, L.-J. Liang, Q. Wang, A. Laaksonen and T. Wu, *Biomater. Sci.*, 2014, **2**, 419-426.
71 F. Müller-Plathe, *ChemPhysChem*, 2002, **3**, 754-769.
72 A. Lazutin, M. Glagolev, V. Vasilevskaya and A. Khokhlov, *J. Chem. Phys.*, 2014, **140**, 134903.
73 S. De Beer, *Langmuir*, 2014, **30**, 8085-8090.
74 H. Merlitz, G.-L. He, C.-X. Wu and J.-U. Sommer, *Phys. Rev. Lett.*, 2009, **102**, 115702.
75 Y. R. Sliozberg, R. A. Mrozek, J. D. Schieber, M. Kröger, J. L. Lenhart and J. W. Andzelm, *Polymer*, 2013, **54**, 2555-2564.
76 A. Ryzhkov, P. Melenev, C. Holm and Y. L. Raikher, *J. Magn. Magn. Mater.*, 2014, **383**, 277-280.
77 G. C. Claudio, K. Kremer and C. Holm, *J. Chem. Phys.*, 2009, **131**, 094903.
78 B. A. Mann, K. Kremer, O. Lenz and C. Holm, *Macromol. Theory Simul.*, 2011, **20**, 721-734.
79 H. Salahshoor and N. Rahbar, *J. Mech. Behav. Biomed. Mater.*, 2014, **37**, 299-306.
80 D.-W. Yin, M. O. De La Cruz and J. J. De Pablo, *J. Chem. Phys.*, 2009, **131**, 194907.
81 M. Quesada-Pérez and A. Martín-Molina, *Soft Matter*, 2013, **9**, 7086-7094.
82 S. Edgecombe and P. Linse, *Macromolecules*, 2007, **40**, 3868-3875.
83 P. G. De Gennes, *Scaling concepts in polymer physics*, Cornell University Press, 1979.
84 M. Rubinstein, R. H. Colby, A. V. Dobrynin and J.-F. Joanny, *Macromolecules*, 1996, **29**, 398-406.
85 A. V. Dobrynin, R. H. Colby and M. Rubinstein, *Macromolecules*, 1995, **28**, 1859-1871.
86 B. A. Mann, K. Kremer and C. Holm, *Macromol. Symp.*, 2006, **237**, 90-107.
87 J. Li, Z. Suo and J. J. Vlassak, *Soft Matter*, 2014, **10**, 2582-2590.
88 R. Marcombe, S. Cai, W. Hong, X. Zhao, Y. Lapusta and Z. Suo, *Soft Matter*, 2010, **6**, 784-793.
89 H. Li, T. Y. Ng, Y. K. Yew and K. Y. Lam, *Biomacromolecules*, 2004, **6**, 109-120.
90 G. Stoychev, S. Zakharchenko, S. Turcaud, J. W. C. Dunlop and L. Ionov, *ACS Nano*, 2012, **6**, 3925-3934.
91 E. C. Achilleos, K. N. Christodoulou and I. G. Kevrekidis, *Comput. Theor. Polym. Sci.*, 2001, **11**, 63-80.
92 W. Guo, M. Li and J. Zhou, *Smart Mater. Struct.*, 2013, **22**, 115028.
93 T. Wallmersperger, A. Attaran, K. Keller, J. Brummund, M. Guenther and G. Gerlach, in *Intelligent Hydrogels*, Springer, 2013, pp. 189-204.
94 Y. Mori, H. Chen, C. Micek and M. Calderer, *SIAM J. Appl. Math.*, 2013, **73**, 104-133.
95 H. Li, *Int. J. Solids Struct.*, 2009, **46**, 1326-1333.
96 H. Li, R. Luo, E. Birgersson and K. Y. Lam, *J. Mech. Phys. Solids*, 2009, **57**, 369-382.
97 D. Li, H. Yang and H. Emmerich, *Colloid Polym. Sci.*, 2011, **289**, 513-521.
98 W. Hong and X. Wang, *J. Mech. Phys. Solids*, 2013, **61**, 1281-1294.
99 Z. Duan, J. Zhang, Y. An and H. Jiang, *J. Appl. Mech.*, 2013, **80**, 041017.
100 Z. G. Mills, W. Mao and A. Alexeev, *Trends Biotechnol.*, 2013, **31**, 426-434.
101 P. Dayal, O. Kuksenok and A. C. Balazs, *Soft Matter*, 2010, **6**, 768-773.
102 M. Ostoja-Starzewski, *Appl. Mech. Rev.*, 2002, **55**, 35-60.
103 G. A. Buxton, C. M. Care and D. J. Cleaver, *Modell. Simul. Mater. Sci. Eng.*, 2001, **9**, 485-497.
104 H. Masoud, B. I. Bingham and A. Alexeev, *Soft Matter*, 2012, **8**, 8944-8951.
105 G. A. Buxton and A. C. Balazs, *J. Chem. Phys.*, 2002, **117**, 7649-7658.
106 V. V. Yashin and A. C. Balazs, *Science*, 2006, **314**, 798-801.
107 R. Yoshida and T. Ueki, *NPG Asia Mater.*, 2014, **6**.
108 I. R. Epstein, V. K. Vanag, A. C. Balazs, O. Kuksenok, P. Dayal and A. Bhattacharya, *Acc. Chem. Res.*, 2011, **45**, 2160-2168.
109 R. Yoshida, T. Takahashi, T. Yamaguchi and H. Ichijo, *J. Am. Chem. Soc.*, 1996, **118**, 5134-5135.
110 Y. Shiraki and R. Yoshida, *Angew. Chem. Int. Ed.*, 2012, **51**, 6112-6116.
111 S. R. Pullela, Q. Wang and Z. Cheng, *Adv. Nanopart.*, 2013, **2**, 94-98.
112 O. Kuksenok, D. Deb, X. Yong and A. C. Balazs, *Mater. Today*, 2014, **17**, 486-493.
113 P. Dayal, O. Kuksenok and A. C. Balazs, *Langmuir*, 2009, **25**, 4298-4301.
114 S. Succi, *The lattice Boltzmann equation: for fluid dynamics and beyond*, Oxford University Press, 2001.
115 A. Ladd and R. Verberg, *J. Stat. Phys.*, 2001, **104**, 1191-1251.

116 S. Chen and G. D. Doolen, *Annu. Rev. Fluid Mech.*, 1998, **30**, 329-364.
117 C. K. Aidun and J. R. Clausen, *Annu. Rev. Fluid Mech.*, 2010, **42**, 439-472.
118 A. Alexeev, R. Verberg and A. C. Balazs, *Macromolecules*, 2005, **38**, 10244-10260.
119 G. A. Buxton, R. Verberg, D. Jasnow and A. C. Balazs, *Phys. Rev. E*, 2005, **71**, 056707.
120 A. Alexeev, R. Verberg and A. C. Balazs, *Phys. Rev. Lett.*, 2006, **96**, 148103.
121 D. L. Ermak and J. A. Mccammon, *J. Chem. Phys.*, 1978, **69**, 1352-1360.
122 J. C. Chen and A. S. Kim, *Adv. Colloid Interface Sci.*, 2004, **112**, 159-173.
123 S. C. Glotzer and W. Paul, *Annu. Rev. Mater. Res.*, 2002, **32**, 401-436.
124 Y. Masubuchi, J.-I. Takimoto, K. Koyama, G. Ianniruberto, G. Marrucci and F. Greco, *J. Chem. Phys.*, 2001, **115**, 4387-4394.
125 H. Pei, S. Allison, B. M. Haynes and D. Augustin, *J. Phys. Chem. B*, 2008, **113**, 2564-2571.
126 M. Kvarnström, A. Westergård, N. Lorén and M. Nydén, *Phys. Rev. E*, 2009, **79**, 016102.
127 Y. Masubuchi, T. Uneyama, H. Watanabe, G. Ianniruberto, F. Greco and G. Marrucci, *J. Chem. Phys.*, 2010, **132**, 134902.
128 R. Kekre, J. E. Butler and A. J. C. Ladd, *Phys. Rev. E*, 2010, **82**, 011802.
129 R. Verberg, A. Alexeev and A. C. Balazs, *J. Chem. Phys.*, 2006, **125**, 224712.
130 A. J. Ladd, *Phys. Rev. Lett.*, 1993, **70**, 1339-1342.
131 O. B. Usta, A. J. Ladd and J. E. Butler, *J. Chem. Phys.*, 2005, **122**, 094902.
132 P. Hoogerbrugge and J. Koelman, *Europhys. Lett.*, 1992, **19**, 155-160.
133 I. V. Pivkin and G. E. Karniadakis, *Phys. Rev. Lett.*, 2008, **101**, 118105.
134 A. Alexeev, W. E. Uspal and A. C. Balazs, *ACS Nano*, 2008, **2**, 1117-1122.
135 C. P. Lowe, *Europhys. Lett.*, 1999, **47**, 145-151.
136 F. Aydin, P. Ludford and M. Dutt, *Soft Matter*, 2014, **10**, 6096-6108.
137 P. Español and P. Warren, *Europhys. Lett.*, 1995, **30**, 191-196.
138 I. V. Pivkin and G. E. Karniadakis, *J. Chem. Phys.*, 2006, **124**, 184101.
139 Z. Li, X. Bian, B. Caswell and G. E. Karniadakis, *Soft Matter*, 2014, **10**, 8659-8672.
140 V. Symeonidis, G. E. Karniadakis and B. Caswell, *Phys. Rev. Lett.*, 2005, **95**, 076001.
141 L. Verlet, *Phys. Rev.*, 1967, **159**, 98-103.
142 L. Verlet, *Phys. Rev.*, 1968, **165**, 201-214.
143 R. B. Bird, P. J. Dotson and N. L. Johnson, *J. Non-Newtonian Fluid Mech.*, 1980, **7**, 213-235.
144 R. E. Van Vliet, H. C. Hoefsloot and P. D. Iedema, *Polymer*, 2003, **44**, 1757-1763.
145 A. Schlijper, P. Hoogerbrugge and C. Manke, *J. Rheol.*, 1995, **39**, 567-579.
146 X. Yong, O. Kuksenok, K. Matyjaszewski and A. C. Balazs, *Nano Lett.*, 2013, **13**, 6269-6274.
147 H. Masoud and A. Alexeev, *Macromolecules*, 2010, **43**, 10117-10122.
148 K. Kremer and G. S. Grest, *J. Chem. Phys.*, 1990, **92**, 5057-5086.
149 G. S. Grest and K. Kremer, *Phys. Rev. A*, 1986, **33**, 3628-3631.
150 G. S. Grest, K. Kremer and T. Witten, *Macromolecules*, 1987, **20**, 1376-1383.
151 Y. R. Sliozberg and J. W. Andzelm, *Chem. Phys. Lett.*, 2012, **523**, 139-143.
152 Y. R. Sliozberg and T. L. Chantawansri, *J. Chem. Phys.*, 2013, **139**, 194904.
153 H. Sun, *J. Phys. Chem. B*, 1998, **102**, 7338-7364.
154 M. Somasi, B. Khomami, N. J. Woo, J. S. Hur and E. S. Shaqfeh, *J. Non-Newtonian Fluid Mech.*, 2002, **108**, 227-255.
155 J. F. Marko and E. D. Siggia, *Macromolecules*, 1995, **28**, 8759-8770.
156 P. T. Underhill and P. S. Doyle, *J. Rheol.*, 2006, **50**, 513-529.
157 A. Cohen, *Rheol. Acta*, 1991, **30**, 270-273.
158 R. Radhakrishnan and P. T. Underhill, *Soft Matter*, 2012, **8**, 6991-7003.
159 R. G. Larson, *Mol. Phys.*, 2004, **102**, 341-351.
160 W. Hennink and C. Van Nostrum, *Adv. Drug Delivery Rev.*, 2012, **64**, 223-236.
161 E. Huisman, T. V. Dillen, P. Onck and E. V. D. Giessen, *Phys. Rev. Lett.*, 2007, **99**, 208103.
162 D. A. Head, A. J. Levine and F. C. Mackintosh, *Phys. Rev. Lett.*, 2003, **91**, 108102.
163 H. Tobita and A. E. Hamielec, *Macromolecules*, 1989, **22**, 3098-3105.
164 A. Gavrilov and A. Chertovich, *Polym. Sci., Ser. A*, 2014, **56**, 90-97.
165 A. Gavrilov, D. Guseva, Y. V. Kudryavtsev, P. Khalatur and A. Chertovich, *Polym. Sci., Ser. A*, 2011, **53**, 1207-1216.
166 P.-H. Lin and R. Khare, *Macromolecules*, 2009, **42**, 4319-4327.
167 T. W. Sirk, K. S. Khare, M. Karim, J. L. Lenhart, J. W. Andzelm, G. B. Mckenna and R. Khare, *Polymer*, 2013, **54**, 7048-7057.
168 G. Buxton, *Europhys. Lett.*, 2008, **84**, 26006.
169 Y. Termonia and P. Smith, *Macromolecules*, 1988, **21**, 2184-2189.
170 G. A. Buxton and N. Clarke, *Phys. Rev. Lett.*, 2007, **98**, 238103.
171 J. Kang, R. L. Steward, Y. Kim, R. S. Schwartz, P. R. Leduc and K. M. Puskar, *J. Theor. Biol.*, 2011, **274**, 109-119.
172 F. Tanaka and S. Edwards, *J. Non-Newtonian Fluid Mech.*, 1992, **43**, 247-271.
173 F. Tanaka and S. Edwards, *Macromolecules*, 1992, **25**, 1516-1523.
174 F. Tanaka and S. Edwards, *J. Non-Newtonian Fluid Mech.*, 1992, **43**, 273-288.
175 T. L. Chantawansri, T. W. Sirk and Y. R. Sliozberg, *J. Chem. Phys.*, 2013, **138**, 024908.
176 T. Jiang, L. Wang and J. Lin, *Langmuir*, 2013, **29**, 12298-12306.
177 Y. Mai and A. Eisenberg, *Chem. Soc. Rev.*, 2012, **41**, 5969-5985.
178 Y. R. Sliozberg, J. W. Andzelm, J. K. Brennan, M. R. Vanlandingham, V. Pryamitsyn and V. Ganesan, *J. Polym. Sci., Part B: Polym. Phys.*, 2010, **48**, 15-25.
179 Y. Sliozberg, K. Strawhecker, J. Andzelm and J. Lenhart, *Soft Matter*, 2011, **7**, 7539-7551.
180 W. X. Pan, D. A. Fedosov, G. E. Karniadakis and B. Caswell, *Phys. Rev. E*, 2008, **78**, 046706.
181 R. D. Groot, in *Novel Methods in Soft Matter Simulations*, Springer, 2004, vol. 640, pp. 5-38.

182 M. Heskins and J. E. Guillet, *J. Macromol. Sci., Chem.*, 1968, **2**, 1441-1455.
183 R. Pelton, *J. Colloid Interface Sci.*, 2010, **348**, 673-674.
184 L.-W. Xia, R. Xie, X.-J. Ju, W. Wang, Q. Chen and L.-Y. Chu, *Nat. Commun.*, 2013, **4**, 2226.
185 R. A. Siegel and B. A. Firestone, *Macromolecules*, 1988, **21**, 3254-3259.
186 H. Du, R. Wickramasinghe and X. Qian, *J. Phys. Chem. B*, 2010, **114**, 16594-16604.
187 S. K. De, N. Aluru, B. Johnson, W. Crone, D. J. Beebe and J. Moore, *J. Microelectromech. Syst.*, 2002, **11**, 544-555.
188 Z. Posel, Z. Limpouchová, K. Šindelka, M. Lísal and K. Procházka, *Macromolecules*, 2014, **47**, 2503-2514.
189 N. K. Li, W. H. Fuss and Y. G. Yingling, *Macromol. Theory Simul.*, 2015, **24**, 7-12.
190 R. D. Groot and K. Rabone, *Biophys. J.*, 2001, **81**, 725-736.
191 D. A. Fedosov, I. V. Pivkin and G. E. Karniadakis, *J. Comput. Phys.*, 2008, **227**, 2540-2559.
192 R. H. Ewoldt, A. Hosoi and G. H. Mckinley, *J. Rheol.*, 2008, **52**, 1427-1458.
193 J. Laurer, S. Khan, R. Spontak, M. Satkowski, J. Grothaus, S. Smith and J. Lin, *Langmuir*, 1999, **15**, 7947-7955.
194 T. W. Sirk, Y. R. Slizoberg, J. K. Brennan, M. Lisal and J. W. Andzelm, *J. Chem. Phys.*, 2012, **136**, 134903.
195 S. Sanchez, A. A. Solovev, Y. Mei and O. G. Schmidt, *J. Am. Chem. Soc.*, 2010, **132**, 13144-13145.
196 W. Gao, S. Sattayasamitsathit, K. M. Manesh, D. Weihs and J. Wang, *J. Am. Chem. Soc.*, 2010, **132**, 14403-14405.
197 J. Kim, M. J. Serpe and L. A. Lyon, *Angew. Chem. Int. Ed.*, 2005, **44**, 1333-1336.
198 G. H. Kwon, G. S. Jeong, J. Y. Park, J. H. Moon and S.-H. Lee, *Lab Chip*, 2011, **11**, 2910-2915.
199 S. V. Nikolov, P. D. Yeh and A. Alexeev, *ACS Macro Lett.*, 2014, **4**, 84-88.
200 D. Schmaljohann, *Adv. Drug Delivery Rev.*, 2006, **58**, 1655-1670.
201 J. Dubbert, T. Honold, J. S. Pedersen, A. Radulescu, M. Drechsler, M. Karg and W. Richtering, *Macromolecules*, 2014, **47**, 8700-8708.
202 J. Dubbert, K. Nothdurft, M. Karg and W. Richtering, *Macromol. Rapid Commun.*, 2014, **36**, 159-164.
203 G. Liu, C. Zhu, J. Xu, Y. Xin, T. Yang, J. Li, L. Shi, Z. Guo and W. Liu, *Colloids Surf., B*, 2013, **111**, 7-14.
204 K. T. Nguyen and J. L. West, *Biomaterials*, 2002, **23**, 4307-4314.
205 B. V. Slaughter, S. S. Khurshid, O. Z. Fisher, A. Khademhosseini and N. A. Peppas, *Adv. Mater.*, 2009, **21**, 3307-3329.
206 M. Krogsgaard, M. A. Behrens, J. S. Pedersen and H. Birkedal, *Biomacromolecules*, 2013, **14**, 297-301.
207 J. L. Hill-West, S. M. Chowdhury, M. J. Slepian and J. A. Hubbell, *Proc. Natl. Acad. Sci. U. S. A.*, 1994, **91**, 5967-5971.
208 K. S. Bohl Masters, E. A. Lipke, E. E. Rice, M. S. Liel, H. A. Myler, C. Zygourakis, D. A. Tulis and J. L. West, *J. Biomater. Sci., Polym. Ed.*, 2005, **16**, 659-672.
209 S. Moeinzadeh and E. Jabbari, *J. Phys. Chem. B*, 2012, **116**, 1536-1543.
210 A. C. Brown, S. E. Stabenfeldt, B. Ahn, R. T. Hannan, K. S. Dhada, E. S. Herman, V. Stefanelli, N. Guzzetta, A. Alexeev and W. A. Lam, *Nat. Mater.*, 2014, **13**, 1108-1114.

